Long-runout landslides and the long-lasting effects of early water activity on Mars

Jessica A. Watkins[1]*, Bethany L. Ehlmann[2,3]*, and An Yin[1]*
[1]Department of Earth, Planetary, and Space Sciences and Institute of Planets and Exoplanets (iPLEX), University of California–Los Angeles, Los Angeles, California 90095-1567, USA
[2]Division of Geological & Planetary Sciences, California Institute of Technology, Pasadena, California 91125, USA
[3]Jet Propulsion Laboratory, California Institute of Technology, Pasadena, California 91109, USA

ABSTRACT

Long-runout subaerial landslides (>50 km) are rare on Earth but are common features shaping Mars' Valles Marineris troughs. In this study, we investigated the highly debated emplacement mechanisms of these Martian landslides by combining spectral and satellite-image analyses. Our results suggest that hydrated silicates played a decisive role in facilitating landslide transport by lubricating the basal sliding zone. This new understanding implies that clay minerals, generated as a result of water-rock interactions in the Noachian and Hesperian (4.1–3.3 Ga), exert a long-lasting influence on geomorphic processes that shape the surface of the planet.

INTRODUCTION

Although landsliding is among the most prominent processes shaping the surfaces of solar system bodies, its emplacement mechanisms both on Earth (e.g., Erismann, 1979; Legros, 2002) and other planets (e.g., Melosh, 1987) remain contentious. An example is the debate over the transport mechanisms of long-runout (>50 km) landslides in the ≤700-km-wide and ≤7-km-deep Valles Marineris (VM) trough system on Mars. Current hypotheses appeal variously to basal lubrication by water, trapped air, ice, snow, evaporates, and dry granular flow (e.g., Lucchitta, 1978; Harrison and Grimm, 2003; McEwen, 1989). Because landslides with shared morphologies occurred widely and nearly continuously from 3 Ga to 50 Ma (Quantin et al., 2004) (Figs. 1A and 1B), resolving the mechanisms of their emplacement may have several important implications for past Mars surface conditions. For example, the involvement of ice (Lucchitta, 1978; De Blasio, 2011) or water (Harrison and Grimm, 2003) at the base of VM landslides could correlate landsliding with wetter, cold or warm climates, respectively, whereas dry granular flow requires no such correlation (McEwen, 1989; Soukhovitskaya and Manga, 2006).

Thus far, efforts in differentiating the competing hypotheses have focused on the geometric properties of VM landslides. These include (1) the ratio of landslide volume to transport distance (McEwen, 1989; Soukhovitskaya and Manga, 2006), (2) multidimensional simulations of landform generation (Harrison and Grimm, 2003; Lucas et al., 2011), (3) surface morphology comparisons to long-runout terrestrial analogs (Lucchitta, 1978; De Blasio, 2011), and (4) the slope and relief of the source (Lajeunesse et al., 2006). These geometric observations have been used to support both dry and wet models.

However, the mineralogic composition of the basal sliding layers of VM landslides has never been directly examined with spectral data.

In this study, we survey the structural relationships and mineral composition of the best-exposed and best-imaged basal section of a long-runout (>75 km) VM landslide (Fig. 1B) using integrated Compact Reconnaissance Imaging Spectrometer for Mars (CRISM) (Murchie et al., 2007), Thermal Emission Imaging System (THEMIS) (Christensen et al., 2004), Context Camera (CTX) (Malin et al., 2007), and High Resolution Science Imaging Experiment (HiRISE) (McEwen et al., 2007) data (see the GSA Data Repository[1] for methods). Our results suggest that transport was facilitated by hydrated silicates in the basal sliding zone, documenting the effects of clay minerals in shaping the morphology of Mars.

Regional Context

A characteristic surface morphology is exhibited by many long-runout VM landslides of diverse ages (Lucchitta, 1978; Quantin et al., 2004). For example, Ius Labes, dated as 100 Ma by crater counting estimate (Quantin et al., 2004), consists of a breakaway zone, an inner zone with tilted blocks (~4 km wide), and an outer zone with a fan-shaped lobe marked by surficial longitudinal grooves (Figs. 1B and 1C). The width of the unconfined outer zone (~43 km) is nearly double that of the inner zone (~28 km, similar to that of the breakaway escarpment), thus requiring significant lateral spreading during landslide runout and an unusual transport mechanism (e.g., Legros, 2002).

Approximately 30 characteristic long-runout landslides occur in VM and of these, 10 had CRISM coverage (Fig. 1A). Among them, five clearly show the presence of clay minerals in materials entrained in their long-runout portions, where dust cover is low and erosion has exposed entrained material at the surface (Fig. 1A; see the Data Repository for additional spectra). Structural relationships between CRISM-detected clay minerals and slide units are rarely discernible due to the concealing nature of later-emplaced stratigraphic units. However, one landslide, Ius Labes (Figs. 1B and 1C), had exemplary exposure of pristine slide deposits due to erosion, and several CRISM full-resolution target (FRT) data covering multiple portions of the deposit permit detailed coupled structural-mineralogic analysis.

GEOLOGIC AND MINERAL MAPPING

We mapped the following geomorphic features and geologic units at the eroded landslide toe and its neighboring region (Figs. 1B and 2A; see the Data Repository): (1) a landslide deposit with a lumpy surface (unit 1 in Fig. 2B), (2) a layered and mesa-forming unit (feature *a* in Fig. 2B) mostly covered by dust and sand dunes, (3) a layered unit with high-albedo patches (feature *b*), crosscut by discontinuous (feature *c*) and degraded (feature *d*) longitudinal grooves, linear and curvilinear scarps, and narrow troughs sub-perpendicular to the grooves (feature *e*), (4) a low-albedo layered unit characterized and crosscut by continuous and well-preserved longitudinal grooves (feature *f*), and transverse extensional cracks (feature *g*), (5) talus deposits from the southern wall, and (6) a young debris-flow sheet overriding the talus deposits. The high- and low-albedo grooved units (i.e., units 3 and 4 in Fig. 2B) are parts of the Ius Labes outer zone; the former (unit 3) is thrust over unit 2, as indicated by a truncated crater basin (feature *h* in Fig. 2B) below the contact. A HiRISE image shows that low-albedo unit 4 is a subhorizontal sheet and overlies high-albedo unit 3 (white arrows in Fig. 2C point to contact). Pervasive parallel grooves, interpreted as stretching lineations, and linear fissures, interpreted as tension gashes (Figs. 2A–2C), in units 3 and 4 are indicative of shared differential shear and lateral spreading at high velocities (>50 m/s for terrestrial examples) during landslide emplacement
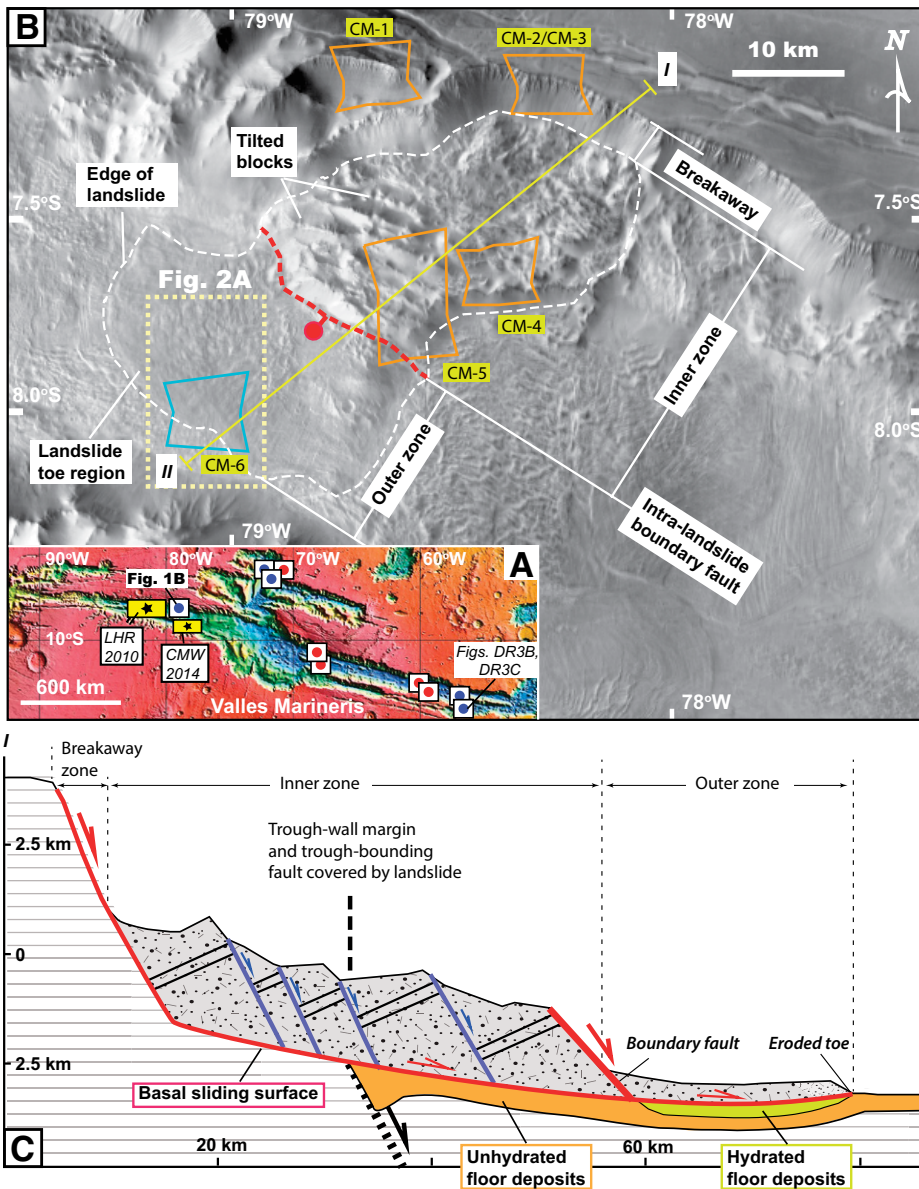

Figure 1. A: Valles Marineris, Mars, showing locations of B, Figure DR3B, and Figure DR3C (see footnote 1), and study areas of Roach et al. (2010; labeled LHR 2010) and Weitz et al. (2014; labeled CMW 2014). Blue circles indicate clays detected in Valles Marineris long-runout landslides; red circles indicate hydrated minerals not detected in landslide. B: Thermal Emission Imaging System daytime infrared mosaic displaying Ius Labes landslides and locations of C and Figure 2A (for regional map, see the Data Repository). Blue box indicates hydrated mineral detection; orange boxes indicate no detectable hydrated minerals. C: Geologic cross section with topographic profile derived from Mars Orbiter Laser Altimeter data.

(McEwen, 1989). The contact and crosscutting relationships between the mapped units are summarized in Figure 2D.

Our analysis of the six available CRISM images reveals no hydrated minerals in the trough-wall breakaway zone, the inner zone, most of the outer zone, and a small outcrop of trough-floor sediments (i.e., unit 2) (Figs. 1B and 2A). In contrast, unit 3 in the landslide basal layer contains hydrated minerals, indicated by absorption bands at 1.4 and 1.9 μm (e.g., Roach et al., 2010). CRISM data from some patches display a sharp doublet, with minima at ~2.21

and ~2.278 μm, and an inflection near 2.4 μm (Fig. 2E), consistent with a hydrated silicate material previously identified at other sites in VM, likely representing a mixture of hydrated silica, Fe-smectite, and/or jarosite (Roach et al., 2010; Weitz et al., 2014; Thollot et al., 2012). Other patches also show absorptions at 2.3 μm (Fig. 2E), characteristic of Fe/Mg-OH in phyllosilicates, which have also been found in VM (Murchie et al., 2009; Roach et al., 2010; Weitz et al., 2014; Thollot et al., 2012) and elsewhere on Mars (Ehlmann et al., 2011). The longitudinal grooves in unit 3 (feature c in Fig. 2B) cross-

cut both high-albedo hydrated silicate patches and low-albedo phyllosilicate patches.

DISCUSSION AND CONCLUSIONS

The longitudinal grooves on the Ius Labes surface are similar to the morphology of exceptional terrestrial landslides, as well as fluidized crater ejecta, possibly lubricated at the base by low-friction ice or snow (Peulvast et al., 2001; De Blasio, 2011; Lucchitta, 1978). Thus, it is conceivable that Ius Labes may have ridden over a layer of ice. However, the lack of compelling morphologic features related to near-surface ice or a periglacial environment, e.g., pingos or polygonal patterned ground (e.g., Soare et al., 2005), does not uniquely implicate this hypothesis. Had Ius Labes instead ridden on top of a water-saturated bed, the landslide would have bulldozed soft materials near its rim outward and created a small-scale fold-and-thrust belt at the landslide front (Dahlen, 1990), and this is not observed.

Instead, the presence of hydrated silicates in the basal layer of this and other landslides suggests that clay minerals may have played a key role in the formation of long-runout landslide morphologies. One such mechanism is lowering the basal friction and thus facilitating long-distance transport. For example, smectite clay absorbs water into its layered crystal structure and can have a friction coefficient that is lower by a factor of three versus that of dry rocks (Saffer and Marone, 2003; Byerlee, 1978). The coefficient of friction is fundamentally dependent on the normal stress on the sliding surface (Byerlee, 1978). We estimate a normal stress of ~15 MPa initially exerted at the landslide base (Hungr and Evans, 2004; for methods, see the Data Repository), yielding a low coefficient of friction of ~0.25 for smectite (Saffer and Marone, 2003), as compared to ~0.85 for igneous rock (Byerlee, 1978). This smectite friction coefficient is consistent with values previously determined for VM landslides (McEwen, 1989). Based on the observed CRISM absorption band strengths, smectite is likely to comprise far less than half of the basal layer's bulk composition. However, as shown by Collettini et al. (2009), even 10% smectite in a mixture under high shear strain yields a bulk friction coefficient similar to that of smectite alone. This is because high shear strain creates interconnected networks of smectite-bearing, low-friction slip surfaces that bound the high-friction material, facilitating long runout. Although the composition of the basal layer surface can only be directly examined at the toe, we expect that mechanically significant hydrated materials are present at the base of most of the landslide mass, based on along-strike projection of regional geology. Directly west and southeast of our study area (yellow boxes in Fig. 1A), Roach et al. (2010) and Weitz et al. (2014),
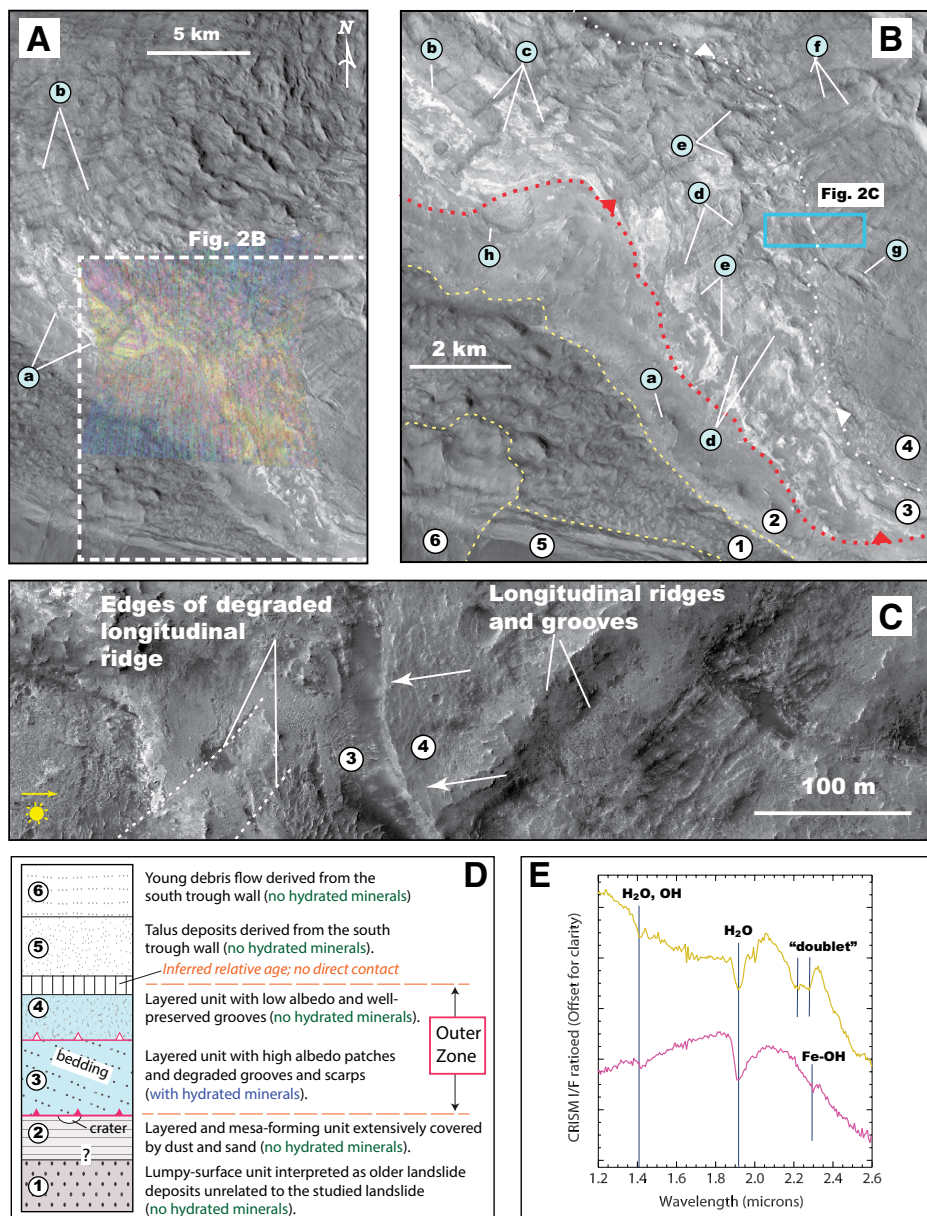
Figure 2. A: Summary spectral parameter map of Compact Reconnaissance Imaging Spectrometer for Mars (CRISM) full-resolution target image FRT0000B939 (R: BD1900, G: Doub2200, B: D2300), where Fe/Mg smectites are magenta; doublet hydrated material is yellow-green; anhydrous materials are dark blue, overlain on Context Camera (CTX) image P07_003606_1727_XN_07S079W (see Fig. 1B for location). Features: *a*—outer rim of the landslide; *b*—longitudinal ridges and grooves. Location of B is also shown. B: Interpreted geologic map of a basal section of the landslide based on CTX image in A. Numbers and letters indicate lithologic units discussed in the text (for unmarked examples, see the Data Repository [see footnote 1]). Dashed red line is trace of basal sliding surface with triangles on overriding plate; dashed white line is trace of an intralandslide sliding surface separating light-toned unit 3 below from dark-toned unit 4 above; yellow lines are geologic contacts unrelated to emplacement of the studied landslide. Blue box shows location of C. C: High Resolution Science Imaging Experiment image (ESP_016172_1720) showing that unit 4 is above unit 3; yellow arrow is sun illumination direction (see the Data Repository for topographic data). D: Summary of geologic units and their contact relationships as shown in B. E: Ratioed CRISM spectra for image FRT0000B939; spectra colors correspond to mapped units in A.

tial alteration of VM wall rock to clay minerals (Murchie et al., 2009) and the later formation of talus slopes and trough-floor deposits with hydrated silicates during the Noachian and Hesperian (Roach et al., 2010; Weitz et al., 2014) (Fig. 3A); (2) slope failure and rotational sliding of the trough-wall rock downslope as a landslide, which was broken into several large, highly fractured blocks and initially traveled over a high-friction, unhydrated surface (Fig. 3B); (3) concurrently, the frontal landslide mass overrode and entrained the hydrated-silicate–bearing floor deposits, causing further loss of coherence and permitting the landslide outer zone to spread laterally while moving forward over the low-friction surface (Dahlen, 1990) (Fig. 3C). Other VM landslides with detected clay minerals have similar morphology and mobility (e.g., Lajeunesse et al., 2006; Lucas and Mangeney, 2007), suggesting that they may have been generated by a similar process. The lack of detection of clay minerals in the others may be explained by incomplete CRISM coverage of the landslides and lack of exposure combined with relatively small amounts of clay (e.g., ~20% smectite in units traversed by the Curiosity rover was not detected from orbit; Vaniman et al., 2014). The first possibility can be tested by future studies as orbital data acquisition continues.

Our climate-independent clay-lubrication model (Fig. 3) is consistent with the interpretation of Quantin et al. (2004) that the nearly continuous occurrence of VM landslides from 3.5 Ga through 50 Ma has been independent of changing climate conditions. It also implies that, although hydrated silicate minerals were created mostly in the Noachian (4.1–3.7 Ga) on Mars as a result of intense early water-rock interactions (Bibring et al., 2006; Murchie et al., 2009; Ehlmann et al., 2011), the effects of early water are long lasting, manifested in the participation of clay minerals in large-scale geomorphic processes shaping Mars' surface even at present.

REFERENCES CITED

Bibring, J.-P., et al., 2006, Global mineralogical and aqueous Mars history derived from OMEGA/Mars Express data: Science, v. 312, p. 400–404, doi:10.1126/science.1122659.

Byerlee, J., 1978, Friction of rocks: Pure and Applied Geophysics, v. 116, p. 615–626, doi:10.1007/BF00876528.

Christensen, P.R., et al., 2004, The Thermal Emission Imaging System (THEMIS) for the Mars 2001 Odyssey Mission: Space Science Reviews, v. 110, p. 85–130, doi:10.1023/B:SPAC.0000021008.16305.94.

Collettini, C., Niemeijer, A., Viti, C., and Marone, C., 2009, Fault zone fabric and fault weak-

respectively, documented trough-floor deposits that contain the same smectite and smectite-jarosite-silica mixture as found in the basal unit of Ius Labes. This particular floor unit (Witbeck et al., 1991) is located directly below the Ius Labes landslide complex.

Based on the preceding arguments, in conjunction with previous understanding of Ius Chasma wall-rock stratigraphy and geologic history (e.g., Murchie et al., 2009; Roach et al., 2010), we propose the following sequence of events to form long-runout landslides: (1) par-
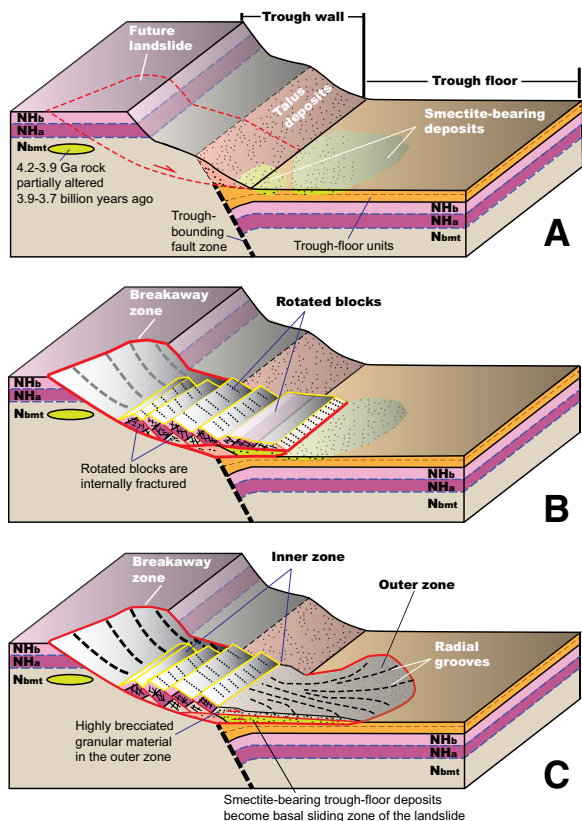
Figure 3. A: Idealized model illustrating clay minerals such as smectite were produced by alteration of trough-wall rocks, and hydrated detritus was later transported to the trough floor. Trough-wall geologic units after Witbeck et al. (1991): N_{bmt} are Noachian basement rocks, locally altered to smectite-bearing hydrated material (Murchie et al., 2009); NH_a and NH_b are Late Noachian–Hesperian volcanic flows that postdate the Noachian alteration event. B: Failed trough-wall rock slides downslope as a landslide. C: Frontal landslide mass rides over low-friction clay-bearing deposits, facilitating long-distance transport.

ness: Nature, v. 462, p. 907–910, doi:10.1038/nature08585.

Dahlen, F.A., 1990, Critical taper model of fold-and-thrust belts and accretionary wedges: Annual Review of Earth and Planetary Sciences, v. 18, p. 55–99, doi:10.1146/annurev.ea.18.050190.000415.

De Blasio, F.V., 2011, Landslides in Valles Marineris (Mars): A possible role of basal lubrication by sub-surface ice: Planetary and Space Science, v. 59, p. 1384–1392, doi:10.1016/j.pss.2011.04.015.

Ehlmann, B.L., Mustard, J.F., Murchie, S.L., Bibring, J.-P., Meunier, A., Fraeman, A.A., and Langevin, Y., 2011, Subsurface water and clay mineral formation on early Mars: Nature, v. 479, p. 53–60, doi:10.1038/nature10582.

Erismann, T.H., 1979, Mechanisms of large landslides: Rock Mechanics, v. 12, p. 15–46, doi:10.1007/BF01241087.

Harrison, K.P., and Grimm, R.E., 2003, Rheological constraints on Martian landslides: Icarus, v. 163, p. 347–362, doi:10.1016/S0019-1035(03)00045-9.

Hungr, O., and Evans, S.G., 2004, Entrainment of debris in rock avalanches: An analysis of a long run-out mechanism: Geological Society of America Bulletin, v. 116, p. 1240–1252, doi:10.1130/B25362.1.

Lajeunesse, E., Quantin, C., Allemand, P., and Delacourt, C., 2006, New insights on the runout of large landslides in the Valles Marineris canyons, Mars: Geophysical Research Letters, v. 33, L04403, doi:10.1029/2005GL025168.

Legros, F., 2002, The mobility of long-runout landslides: Engineering Geology, v. 63, p. 301–331, doi:10.1016/S0013-7952(01)00090-4.

Lucas, A., and Mangeney, A., 2007, Mobility and topographic effects for large Valles Marineris landslides on Mars: Geophysical Research Letters, v. 34, L10201, doi:10.1029/2007GL029835.

Lucas, A., Mangeney, A., Mege, D., and Bouchut, F., 2011, Influence of the scar geometry on landslide dynamics and deposits: Application to Martian landslides: Journal of Geophysical Research, v. 116, E10001, doi:10.1029/2011JE003803.

Lucchitta, B.K., 1978, A large landslide on Mars: Geological Society of America Bulletin, v. 89, p. 1601–1609, doi:10.1130/0016-7606(1978)89<1601:ALLOM>2.0.CO;2.

Malin, M.C., et al., 2007, Context Camera investigation on board the Mars Reconnaissance Orbiter: Journal of Geophysical Research, v. 112, E05S04, doi:10.1029/2006JE002808.

McEwen, A.S., 1989, Mobility of large rock avalanches: Evidence from Valles Marineris, Mars: Geology, v. 17, p. 1111–1114, doi:10.1130/0091-7613(1989)017<1111:MOLRAE>2.3.CO;2.

McEwen, A.S., et al., 2007, Mars Reconnaissance Orbiter's High Resolution Imaging Science Experiment (HiRISE): Journal of Geophysical Research, v. 112, E5S02, doi:10.1029/2005JE002605.

Melosh, H.J., 1987, The mechanics of large rock avalanches: Reviews in Engineering Geology, v. 7, p. 41–50, doi:10.1130/REG7-p41.

Murchie, S.L., et al., 2007, Compact Reconnaissance Imaging Spectrometer for Mars (CRISM) on Mars Reconnaissance Orbiter (MRO): Journal of Geophysical Research, v. 112, E05S03, doi:10.1029/2006JE002682.

Murchie, S.L., et al., 2009, A synthesis of Martian aqueous mineralogy after 1 Mars year of observations from the Mars Reconnaissance Orbiter: Journal of Geophysical Research, v. 114, E00D06, doi:10.1029/2009JE003342.

Peulvast, J.P., Mege, D., Chiciak, J., Costard, F., and Masson, P.L., 2001, Morphology, evolution and tectonics of Valles Marineris wallslopes (Mars): Geomorphology, v. 37, p. 329–352, doi:10.1016/S0169-555X(00)00085-4.

Quantin, C., Allemand, P., Mangold, N., and Delacourt, C., 2004, Ages of Valles Marineris (Mars) landslides and implications for canyon history: Icarus, v. 172, p. 555–572, doi:10.1016/j.icarus.2004.06.013.

Roach, L.H., Mustard, J.F., Swayze, G., Milliken, R.E., Bishop, J.L., Murchie, S.L., and Lichtenberg, K., 2010, Hydrated mineral stratigraphy of Ius Chasma, Valles Marineris: Icarus, v. 206, p. 253–268, doi:10.1016/j.icarus.2009.09.003.

Saffer, D.M., and Marone, C., 2003, Comparison of smectite- and illite-rich gouge frictional properties: Application to the updip limit of the seismogenic zone along subduction megathrusts: Earth and Planetary Science Letters, v. 215, p. 219–235, doi:10.1016/S0012-821X(03)00424-2.

Soare, R.J., Burr, D.M., and Wan Bun Tseung, J.M., 2005, Possible pingos and a periglacial landscape in northwest Utopia Planitia: Icarus, v. 174, p. 373–382, doi:10.1016/j.icarus.2004.11.013.

Soukhovitskaya, V., and Manga, M., 2006, Martian landslides in Valles Marineris: Wet or dry?: Icarus, v. 180, p. 348–352, doi:10.1016/j.icarus.2005.09.008.

Thollot, P., et al., 2012, Most Mars minerals in a nutshell: Various alteration phases formed in a single environment in Noctis Labyrinthus: Journal of Geophysical Research, v. 117, E00J06, doi:10.1029/2011JE004028.

Vaniman, D.T., et al., 2014, Mineralogy of a mudstone at Yellowknife Bay, Gale crater, Mars: Science, v. 343, doi:10.1126/science.1243480.

Weitz, C.M., Dobrea, E.N., and Wray, J.J., 2014, Mixtures of clays and sulfates within deposits in western Melas Chasma, Mars: Icarus, doi:10.1016/j.icarus.2014.04.009.

Witbeck, N.E., Tanaka, K.L., and Scott, D.H., 1991, Geologic map of the Valles Marineris region, Mars: U.S. Geological Survey Miscellaneous Investigation Series Map I-2010, scale 1:2,000,000.

Geology

Long-runout landslides and the long-lasting effects of early water activity on Mars

Jessica A. Watkins, Bethany L. Ehlmann and An Yin

Email alerting services	click www.gsapubs.org/cgi/alerts to receive free e-mail alerts when new articles cite this article
Subscribe	click www.gsapubs.org/subscriptions/ to subscribe to Geology
Permission request	click http://www.geosociety.org/pubs/copyrt.htm#gsa to contact GSA

Notes

THE
GEOLOGICAL
SOCIETY
OF AMERICA